Iranian Journal of Pharmaceutical Research (2020), 19 (2): 207-218
DOI: 10.22037/IJPR.2020.1101026
Received: May 2018
Accepted: January 2019

Original Article

Evaluation of Blood and Liver Cytotoxicity and Apoptosis-necrosis Induced by Nanochelating Based Silver Nanoparticles in Mouse Model

Seyedeh Mahsan Hoseini-Alfatemi[a], Fatemeh Fallah[a], Shahnaz Armin[a], Maryam Hafizi[b, c], Abdollah Karimi[a*] and Somayeh Kalanaky[c*]

[a]*Pediatric Infections Research Center, Research Institute for Children Health, Shahid Beheshti University of Medical Sciences, Tehran, Iran.* [b]*Cancer Research Center, Shahid Beheshti University of Medical Science, Tehran, Iran.* [c]*Department of Research and Development, Sodour Ahrar Shargh Company, Tehran, Iran.*

Abstract

This study aimed to evaluate the *in-vitro* and *in-vivo* biological activities of newly synthesized nanochelating based silver nanoparticles (AgNPs) in mouse model. Nanochelating technology was used to design and synthesize the AgNPs. The animals studies were including the lethal dose (LD50) determination by the intraperitoneal administration in mice, and determination of liver enzymes levels and hematological parameters. Flow cytometry analysis was used to quantitatively determine apoptosis and necrotic cells *in-vitro*. The NPs A and NPs B have LD50 = 250 mg/kg and LD50 = 350 mg/kg, respectively and classified as non-toxic. In general, minor alterations were observed in levels of liver enzymes as indicative of liver damage. For blood parameters several factors associated with significant changes in AgNPs treated animals. Regarding animals weight, combination therapy showed more effective to maintain animals weight losses after infection. Flow cytometry results showed that AgNPs induced cell apoptosis-necrosis depends on AgNP size, concentration and exposure time. Cells damage due to AgNPs (A) with lower size (20-25 nm) were relatively more than cells exposed to AgNPs (B) (30-35 nm). The findings support the potent antibacterial activities of nanochelating based AgNPs. Also, the present study showed that nanochelating based AgNPs induce a moderate level of apoptosis/necrosis in mice, and affected several clinical parameters like blood parameters, liver enzymes, and body weight with no definite signs of toxicity.

Keywords: Silver nanoparticles; Apoptosis; Necrosis; Cellular cytotoxicity; Nanochelating.

Introduction

Hospital-acquired infections (HIs) are a widespread problem that currently presents in healthcare environments, occurring in approximately 4 to 10 percent of hospitalized patients annually (1). Multiple-drug-resistant (MDR) bacteria including methicillin-resistant *Staphylococcus aureus* (MRSA), vancomycin-resistant enterococci (VRE), extended-spectrum beta-lactamase (ESBLs) producing *Enterobacteriaceae*, *Pseudomonas aeruginosa*, and *Acinetobacter baumannii* (*A. baumannii*) are the main causes of HIs (2-6). In the recent years due to uncontrolled

* Corresponding authors:
E-mail: dr.karimiabdollah@gmail.com
skalanaky@nanochelatingtechnology.com

use of antibiotics and development of various antibiotic resistance mechanisms, increasing trend of antibiotic resistance in bacterial strains become one of the major threats to human health (7-9). Moreover, the majority of MDR infections require prolonged antibiotic treatment that is associated with increased hospitalization and health-care costs (10-12).

The antibiotic resistance challenging and dynamic pattern of infectious diseases indicating that there is a serious need to develop new therapeutics options which can overcome drug resistance (13). Non-traditional antibacterial agents such as antibody-based therapeutics and metal-based nanoparticles (NPs) are among the most interesting alternative to overcome the antibiotic resistance problem in pathogenic microorganisms (14). NPs are now considered as a practical alternative to antibiotics and seems to have a high potential capability to solve the emergence of MDR bacteria (15). Antimicrobial NPs offer many distinct advantages in reducing acute toxicity, overcoming resistance, lowering cost, targeted delivery, combinatorial antibiotic delivery, and nanoparticle-based bacterial detection when compared to conventional antibiotics (16). In particular, silver nanoparticles (AgNPs), which has an ancient history as an antimicrobial agent and showed antiseptic and antibacterial properties against a wide range of Gram-positive and -negative bacteria (14, 15).

The use of combination strategies to overcome antibiotic resistance is slowly finding its way as a promising attempt to reduce the number of antibiotics to be administered, generate synergistic effects, and counteract antibiotic resistance (14, 17 and 18). In this regard, NPs offer unique properties to increase combinatorial antibiotic delivery and numerous applications have been studied to address a variety of bacterial infections. For example, NPs capped or in combination with existing antibiotics indicate enhanced antibacterial activities against resistant bacteria compared to antibiotics and NPs alone (16, 19).

Because of the significant increase in antimicrobial resistance among common bacterial pathogens in this study for the first time we investigated the *in-vitro* and *in-vivo* biological activities of newly synthesized nanochelating based AgNPs against infected mice.

Experimental

Synthesis of AgNPs

This *in-vivo* case-control study was performed using Nanochelating based technology provided by the Sodour Ahrar Shargh Co. to design and synthesize the AgNPs, a method for producing chelate compounds was registered at US20120100372A1 in the United States Patent Office (20). Self-assembly method has been applied to produce AgNPs as described previously in our published work (21). Based on electron microscopy assay the mean size of two synthesized AgNPs were about 20-25 nm for NPs (A), and 30-35 nm for NPs (B) (21).

Structural analysis

Structures of two synthesized AgNPs have been investigated by X-Ray Diffraction (XRD) analysis. The dry powder of them are used for XRD analysis. The diffracted intensities were recorded from 20 °C-80 °C at 2 theta angles. XRD analysis was conducted by the Philips X'Pert MPD (Philips, Netherlands) at Tarbiat Modares University.

Evaluation of cytotoxicity

To assess the probable toxicity of synthesized AgNPs standard tests for evaluating the median lethal dose (LD50) were carried out according to the Organization for Economic Co-operation and Development guidelines (OECD, guideline 420) in the School of Pharmacy at Tehran University of Medical Sciences (22, 23).

Bacterial strains

The used strains were a Gram-positive and -negative bacteria including *Staphylococcus aureus* (*S. aureus*) ATCC 25923, and *A. baumannii* ATCC 19606, respectively. All bacterial strains were obtained from the Institute of Pastor Technology (Tehran, Iran). The strains were recovered from stocks by cultured overnight at 37 °C under aerobic conditions in tryptic soy agar (TSA) plates containing 5% defibrinated sheep blood (Merck, Germany).

Animals

Six to eight-weeks-old male Wistar albino rats (Weight 200 ± 10 g) were obtained from the Pasteur Institute of Iran. All the animal

studies were conducted according to the relevant national and international guidelines of Shahid Beheshti University of Medical Sciences (24). All the mice were maintained in large group houses under temperature 25 ± 2 °C and 12-hour dark/light cycles with proper access to food and water.

In-vivo experimental design

Animals were divided into 22 groups, 6 mice in each group. Mice were shaved on the back and injected intradermally with 10 µL of *S. aureus* (groups A1 to F1) and *A. baumannii* (A2 to F2) with a final concentration of 1×10^7 CFUs using a sterile insulin syringe. At 24 h after the first injection, mice treated with 0.1 mg kg^{-1} and 0.01 mg kg^{-1} NPs alone and simultaneously with vancomycin (1 mg kg^{-1}) and colistin (15 mg kg^{-1}) via intravenous injection (tail vein) (25). The vancomycin, and colistin antibiotics powder purchased from Sigma-Aldrich, USA. At first and tenth day of the experiment, blood was drawn from animals and serum was separated by centrifugation (3000 rpm for 20 min). Then, concentrations of liver enzymes, including ALT, and AST were determined using marketed reagent kits (Pars Azmoon, Tehran, Iran). Hematological parameters including white blood cells (WBCs), red blood cells (RBCs), mean corpuscular volume (MCV), mean corpuscular hemoglobin (MCH), red cell distribution width (RDW), platelets (PLT), mean platelet volume (MPV), and platelet distribution width (PDW) were determinate using a BC3000 MINDRAY automated hematology analyzer (Mindray, China). Animals were weighed twice prior of injections and at the end of experiments.

In-vitro cell viability assay

Flow cytometry analysis was used to quantitatively determine apoptosis and necrotic cell population induced by AgNPs in L929 mouse fibroblast cell lines was purchased from the Pasteur Institute, Tehran, Iran (26). Cells were grown as monolayer cultures in Dulbecco's Modified Eagle's Medium (DMEM; Bioidea, Iran), culture medium supplemented with 10% fetal bovine serum (FBS; Gibco, USA), and 1% antibiotics (100 IU/mL penicillin, and 100 µg/mL streptomycin; Bioidea, Iran). Cell lines were maintained at 37 °C with 5% CO2 atmosphere and 95% humidity. Cells were routinely sub-cultured when they reached 80% confluency. The passage number of all used cells was less than 10. Forward scatter characteristics (FSC-A) and side scatter characteristics (SSC-A) plots were used to set up the gates to distinguish between NPs and cells. Briefly, the cells were treated with 0.1 and 0.01 µg/mL AgNPs for 24 and 48 h in a 96-well plate at the density of 10,000 cells per well. After the incubation period, the cells were detached, centrifuged 10 min at 1800 rpm, washed and stained with Annexin V and propidium iodide (PI) using apoptosis detection kit according to the manufacturer's protocol (BD Bioscience, USA) (27). In each panel the lower left quadrant shows cells which are negative for both Annexin V and PI staining, upper left quadrant shows necrotic cells that stained only with PI. The lower right quadrant shows early apoptotic cells stained with Annexin V, and the upper right quadrant shows late apoptosis cells stained with both Annexin V and PI. All analyses were performed on a FACSCalibur (BD Biosciences, USA) flow cytometer. All experiments were performed in duplicate, and the data were analyzed by FlowJo software, version 7.6.1 (Tree Star, USA).

Statistical analysis

The results are presented as descriptive statistics in terms of relative frequency. Values were expressed as the mean ± standard deviation (continuous variables) or percentages of the group (categorical variables). Kruskal-Wallis test and Tukey's post hoc test was used to assess inter-group comparison of variables by SPSS ver. 21.0 (IBM Co., Armonk, NY, USA) software. *P*-value < 0.05 was considered as significant.

Results

LD50 assay

The toxicity report showed that intraperitoneal LD50 of synthesized nanoparticles for mice was 250 mg/kg and 350 mg/kg in A and B, respectively. Thus, these NPs were classified as non-toxic (Figure 1).

XRD characterizations of nanoparticles

As it can be seen in XRD spectrum of sample A in Figure 2, the highest peaks are at angles Θ = 322 and then Θ = 802. These two peaks

Acute toxicity of AgNPs (A) when administrated intraperitoneally to mice

Group A	Dose (mg/Kg)	Mortality (%) After 24 hours	Mortality (%) After 48 hours	Mortality (%) After 72 hours	Mortality (%) Up to 14 days
1	2000	100	0	0	100
2	1000	100	0	0	100
3	500	100	0	0	100
4	400	100	0	0	100
5	350	100	0	0	100
6	300	0	50	25	75
7	250	25	0	25	50
8	200	0	0	25	25
9	180	0	0	0	0

Acute toxicity of AgNPs (B) when administrated intraperitoneally to mice

Group A	Dose (mg/Kg)	Mortality (%) After 24 hours	Mortality (%) After 48 hours	Mortality (%) After 72 hours	Mortality (%) Up to 14 days
1	2000	80	20	0	100
2	1000	60	0	0	100
3	500	60	0	0	100
4	400	60	0	0	100
5	350	0	0	0	50
6	300	0	0	0	50
7	250	0	0	0	50
8	200	0	0	0	0
9	180	0	0	0	0

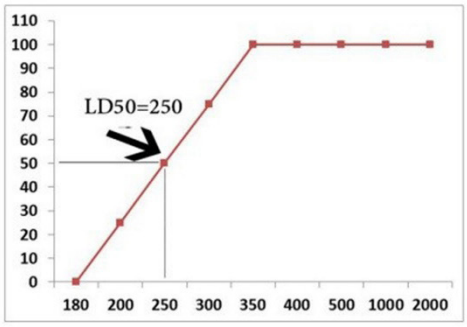

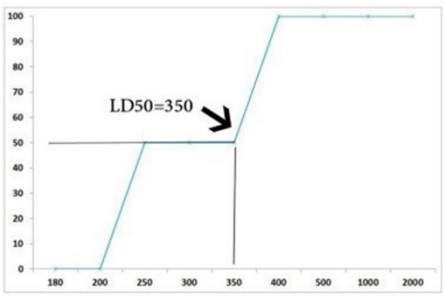

Figure 1. The evaluation of lethal dose (LD50) of AgNPs when administrated intraperitoneal in mic. As it is shown in the graph, nanoparticle A and nanoparticle B have LD50 = 250 mg/kg and LD50 = 350 mg/kg, respectively. This test is done on 9 mice groups of 5 according to protocol of the Organization for Economic Cooperation and Development (OECD).

are distinguishing indices of nano structure A, while in XRD spectrum of sample B, the highest peak is at angle Θ = 352 with a higher intensity than sample A. No peak is observed in the range of Θ = 802. The most important distinguishing indices of these two structures are peak positions Θ = 802 and Θ = 322 in nano structure A, which are absent in nano structure B and also the absence of peaks in the range of Θ = 652 and Θ = 372 in sample A.

The summarized results of XRD analysis

AgNPs Size (nm)	Peak position 2Θ	Reflection
AgNPs (A) (25 nm)	400	32
	280	80
AgNPs (B) (35 nm)	700	37
	550	65

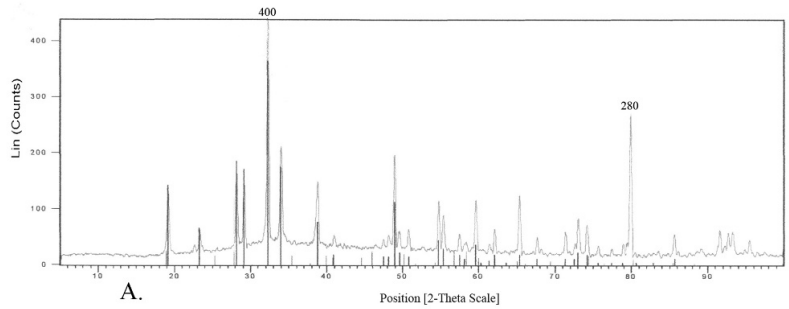

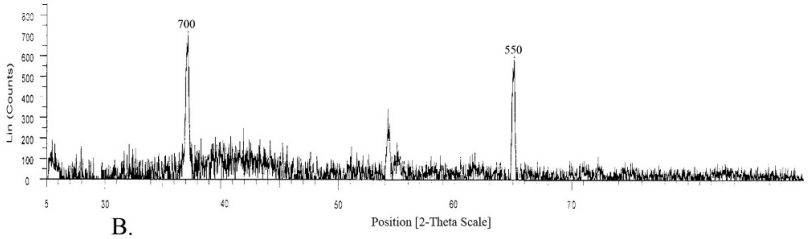

1 - File: X526.raw - Type: 2Th/Th locked - Start: 5.000 ° - End: 70.020 ° - Step: 0.020 ° - Step time: 1 s - Temp.: 25 °C (Room) - Time Started: 5 s - 2-Theta: 5.000 ° - Theta: 2.500 ° - Phi: 0.00 ° - Aux1: 0.0 - Aux2: 0.0

Figure 2. X-Ray diffraction (XRD) analysis of AgNPs. XRD was used to analysis the structure characterization of two synthesized AgNPs. (A) results of AgNPs (A); (B) results of AgNPs (B).

In-vivo assay

In general, minor alterations were observed in clinical chemistry parameters including the level of ALT, and AST as an indicator for liver damages (Table 1). These parameters showed a dose-dependent effect since the elevation of chemistry parameters with reduction of injection dose (0.1 to 0.01 mg kg^{-1}) was decreased. Moreover, significant synergetic effects observed when antibiotics administrated with NPs. A significant lower liver damage was seen in groups treated with AgNPs (A) indicated in their better activity compared to AgNPs (B).

Table 1. Effects of AgNPs treatment on levels of ALT, AST, and weight of studied animals.

Groups	Variables	ALT (Unit/L)		AST (Unit/L)		Weight (gram)	
		1st day	10th day	1st day	10th day	1st day	10th day
A1	SA	15.5 ± 1.3	14.8 ± 0.8	52.2 ± 1.7	55.3 ± 1.2	205.3 ± 2.2	223 ± 3.1
B1a	SA + AgNPs (A) at 0.1 µg/mL	40.8 ± 0.8	39.8 ± 1.2	42.2 ± 1.7	44.7 ± 2.2	208 ± 2.1	201.8 ± 3.8
B1b	SA + AgNPs (B) at 0.1 µg/mL	44.2 ± 0.8	42.7 ± 1	35.5 ± 1.1	37.8 ± 0.8	206 ± 2.2	172.8 ± 4.4
C1a	SA + AgNPs (A) at 0.01 µg/mL	43.8 ± 1.2	46.3 ± 1.6	38.5 ± 1.9	41.2 ± 1.9	205 ± 1.5	170.8 ± 1.9
C1b	SA + AgNPs (B) at 0.01 µg/mL	44.3 ± 0.8	44.5 ± 0.5	37 ± 1.4	33.2 ± 1.5	206.5 ± 2.2	188.5 ± 5.1
D1a	SA + AgNPs (A) at 0.1 µg/mL + vancomycin	35.3 ± 1	37.5 ± 1	23.3 ± 1	26.2 ± 1.2	207.7 ± 1.9	187.5 ± 5
D1b	SA + AgNPs (B) at 0.1 µg/mL + vancomycin	36.2 ± 1.2	36 ± 1.3	27.7 ± 1.6	26.7 ± 1.4	207.7 ± 2.8	176.3 ± 3.4
E1a	SA + AgNPs (A) at 0.01 µg/mL + vancomycin	31.2 ± 1.2	29 ± 1.5	28.7 ± 4.4	31.2 ± 1.7	205 ± 1.4	173.7 ± 5
E1b	SA + AgNPs (B) at 0.01 µg/mL + vancomycin	29.8 ± 1.2	31.8 ± 1.2	28 ± 1.4	29.7 ± 1.2	206.3 ± 1.6	175.3 ± 5
F1	SA + vancomycin	50.8 ± 1.5	53.3 ± 1.9	33 ± 1.4	37 ± 1.4	207.5 ± 2.7	205.3 ± 2.7
G1	Normal saline	11 ± 1	14.2 ± 0.8	17.8 ± 0.8	17.8 ± 1	206.2 ± 2.1	228.2 ± 2.6
A2	AC	21 ± 1	25 ± 0.9	47.3 ± 1.3	49.2 ± 1.7	206.8 ± 2.1	159.7 ± 2.6
B2a	AC + AgNPs (A) at 0.1 µg/mL	26.8 ± 1.2	27.5 ± 1	45.1 ± 1.2	47.5 ± 1.5	207.5 ± 1.9	204.5 ± 2.1
B2b	AC + AgNPs (B) at 0.1 µg/mL	33.8 ± 1.2	36.8 ± 1.2	31.7 ± 1	35.7 ± 0.8	208.2 ± 3	186.7 ± 3.9
C2a	AC + AgNPs (A) at 0.01 µg/mL	17.8 ± 1.5	17 ± 1.4	34 ± 0.9	36.3 ± 1	209 ± 1.8	201.5 ± 2.9
C2b	AC + AgNPs (B) at 0.01 µg/mL	17.7 ± 1.4	15.8 ± 1.2	32.5 ± 1.1	34.8 ± 1.5	210.5 ± 1.9	201.5 ± 2.9
D2a	AC + AgNPs (A) at 0.1 µg/mL + colistin	44.2 ± 1.2	47.8 ± 1.7	31.3 ± 1.2	32.5 ± 1.1	210 ± 2.1	202.7 ± 2.7

Continued Table 1. Effects of AgNPs treatment on levels of ALT, AST, and weight of studied animals.

Groups	Variables	ALT (Unit/L)		AST (Unit/L)		Weight (gram)	
		1st day	10th day	1st day	10th day	1st day	10th day
D2b	AC + AgNPs (B) at 0.1 µg/mL + colistin	50.2 ± 1.5	49.5 ± 1.9	36.2 ± 1.2	38.3 ± 0.8	209.2 ± 1.7	204.5 ± 1
E2a	AC + AgNPs (A) at 0.01 µg/mL + colistin	46 ± 1.1	48.2 ± 1.2	30.7 ± 1.2	34.5 ± 1.4	209.2 ± 2.3	206.8 ± 2.8
E2b	AC + AgNPs (B) at 0.01 µg/mL + colistin	48.3 ± 1.9	51.5 ± 1.6	21.5 ± 1	25 ± 1.4	208.2 ± 2.2	207 ± 2.4
F2	AC + colistin	58.7 ± 1.2	56.5 ± 1.1	41.2 ± 1.2	43.3 ± 1.8	208.7 ± 2.5	205.2 ± 3.2
G2	Normal saline	10.2 ± 0.8	14 ± 0.9	15.9 ± 0.8	15.3 ± 0.5	208.3 ± 2.9	231 ± 3.3

SA: *S. aureus*; AC: *A. baumannii.*

For blood parameters, several factors associated with significant changes in AgNPs treated animals (Table 2). The total number of WBCs was significantly decreased in groups simultaneously experienced AgNPs and antibiotics compared to AgNPs alone, which is indicated by their better healing effect. In RBCs similar to WBCs combination therapy with antibiotics showed better effects. Moreover, in a dose-dependent manner, a lower concentration of AgNPs showed a lower reduction in the total number of RBCs. Regarding to animals weight, combination therapy showed more effective to maintain animals weight losses after infection. In general, it seems that based on statistical analysis results, AgNPs has a more pronounced effect against Gram-positive strains than Gram-negative strains.

Table 2. Effects of AgNPs treatment on hematological parameters of studied animals.

Groups	Variables	WBC ($x10^3$/µL)		RBC ($x10^6$/µL)		RDW (%)		PLT ($x10^3$/µL)		PDW (%)	
		1st day	10th day	1st day	10th day	1st day	10th day	1st day	10th day	1st day	10th day
A1	SA	16.8 ± 1.2	21.3 ± 1.2	4.8 ± 0.3	4.6 ± 0.3	12.8 ± 1.1	10.7 ± 0.2	306.3 ± 4.9	413 ± 7	18.8 ± 0.2	12.2 0.2
B1a	SA + AgNPs (A) at 0.1 µg/mL	11.7 ± 1.2	11.2 ± 0.8	4.8 ± 0.2	4.4 ± 0.3	12.5 ± 1.3	10.1 ± 0.2	307.7 ± 2.1	415.6 ± 2.3	18.6 ± 0.5	12.1 ± 1
B1b	SA + AgNPs (B) at 0.1 µg/mL	10.7 ± 0.5	10.8 ± 0.4	4.9 ± 0.1	4.1 ± 0.2	12.8 ± 1.4	10.1 ± 0.2	311 ± 2.3	4177 ± 2	17.6 ± 0.6	12.2 ± 0.2
C1a	SA + AgNPs (A) at 0.01 µg/mL	10.3 ± 0.5	10.6 ± 0.5	5 ± 0.1	4.2 ± 0.2	12.9 ± 1.4	10.2 ± 0.2	314.5 ± 3	422.2 ± 4.4	19.5 ± 0.4	12.1 ± 0.2
C1b	SA + AgNPs (B) at 0.01 µg/mL	11 ± 0.6	11 ± 0.6	5.5 ± 0.2	4.7 ± 0.1	12.7 ± 1.1	10.5 ± 0.1	318.5 ± 2.1	425 ± 3	17.2 ± 0.4	12.1 ± 1
D1a	SA + AgNPs (A) at 0.1 µg/mL + vancomycin	11.3 ± 0.8	7.5 ± 1	4.7 ± 0.2	4.7 ± 0.1	12.7 ± 1.1	10.3 ± 0.2	190.8 ± 6.9	177.3 ± 7.6	16.2 ± 0.4	12.3 ± 0.2
D1b	SA + AgNPs (B) at 0.1 µg/mL + vancomycin	10.5 ± 0.5	6.8 ± 0.8	4.3 ± 0.1	4.2 0.1	12.8 ± 1.1	10.5 ± 0.2	172 ± 2.8	123.7 3.5	18.5 ± 0.5	12.1 ± 0.1
E1a	SA + AgNPs (A) at 0.01 µg/mL + vancomycin	10.7 ± 0.5	8.3 ± 0.5	4.1 ± 0.1	4.7 0.1	12.7 ± 1.1	10.5 ± 0.2	165.5 ± 8.3	121 4.2	18.5 ± 0.3	12.1 ± 1

Continued Table 2. Effects of AgNPs treatment on hematological parameters of studied animals.

Groups	Variables	WBC ($x10^3$/µL)		RBC ($x10^6$/µL)		RDW (%)		PLT ($x10^3$/µL)		PDW (%)	
		1st day	10th day	1st day	10th day	1st day	10th day	1st day	10th day	1st day	10th day
E1b	SA + AgNPs (B) at 0.01 µg/mL + vancomycin	10.3 ± 0.8	5.5 ± 0.8	4.3 ± 0.1	4.7 ± 0.04	12.8 ± 1.1	10.6 ± 0.1	164.7 ± 3.8	131.2 ± 5.3	18.6 ± 0.2	12.3 ± 0.2
F1	SA + vancomycin	9.8 ± 0.8	7.7 ± 0.5	4 ± 0.04	4.7 ± 0.04	12.6 ± 1.1	10.4 ± 0.1	310.8 ± 4.8	284.7 ± 3.8	18.5 ± 0.6	12.1 ± 0.2
G1	Normal saline	7.7 ± 0.8	7.7 ± 0.8	4.1 ± 0.1	4.7 ± 0.04	12.6 ± 1.1	10.2 ± 0.1	261 ± 4.9	238.3 ± 5.3	12 ± 0.4	12.1 ± 1
A2	AC	10.2 ± 0.4	10 ± 0	5.1 ± 0.1	4.7 ± 0.1	13.2 ± 1.6	10.2 ± 0.2	320 ± 3.3	344.5 ± 4	17.1 ± 0.4	12.2 ± 0.2
B2a	AC + AgNPs (A) at 0.1 µg/mL	10.2 ± 0.4	10 ± 0	5.3 ± 0.1	4.8 ± 0.1	12.6 ± 1.2	10.3 0.2	316.3 ± 3.2	309.3 ± 3	18.5 ± 0.4	12.1 ± 0.1
B2b	AC + AgNPs (B) at 0.1 µg/mL	10.8 ± 0.4	10.8 ± 0.4	4.5 ± 0.1	4.7 ± 0.04	13.1 ± 1.3	10.5 ± 0.2	302 ± 5.5	284 ± 4.6	18.5 ± 0.3	12.1 ± 1
C2a	AC + AgNPs (A) at 0.01 µg/mL	13.8 ± 1	13.7 ± 0	4 ± 0.03	4.7 ± 0	13.1 ± 1.5	10.1 ± 1	264.5 ± 9.2	255.5 ± 10.7	18.1 ± 0.4	12.1 ± 0.1
C2b	AC + AgNPs (B) at 0.01 µg/mL	15.8 ± 0.4	15 ± 1.7	4.3 ± 0.2	4.7 ± 0.1	12.9 ± 1.2	10.4 ± 0.9	249.8 ± 2.7	248.5 ± 2.7	18.1 ± 0.2	12 ± 0.04
D2a	AC + AgNPs (A) at 0.1 µg/mL + colistin	12 ± 0.6	10.2 ± 0.4	3.4 ± 0.1	4.6 ± 0.2	12.7 ± 1.2	10.2v 0.6	156.8 ± 5.3	160.7 ± 5.2	19.4 ± 0.1	12.5 ± 0.1
D2b	AC + AgNPs (B) at 0.1 µg/mL + colistin	12 ± 0	8.2 ± 0.4	3.6 ± 0.1	5 ± 0.5	12.8 ± 1	10.8 ± 0.1	166.3 ± 3.6	161.3 ± 4.5	19.5 ± 0.2	12.3 ± 0.2
E2a	AC + AgNPs (A) at 0.01 µg/mL + colistin	10.7 ± 1	7.3 ± 0.5	4.4 ± 0.1	4.7 ± 0.04	13.1 ± 1.4	10.3 ± 1	187.2 ± 4.2	173.2 ± 5.4	19.1 ± 0.5	12.3 ± 1
E2b	AC + AgNPs (B) at 0.01 µg/mL + colistin	10.8 ± 0.4	5.2 ± 1	4.6 ± 0.1	4.7 ± 0.1	13.1 ± 1	10.9 ± 0.1	180.7 ± 5.3	177.5 ± 5.4	19.1 ± 0.2	12.1 ± 1
F2	AC + colistin	10.2 ± 0.4	10 ± 0	4.2 ± 0.3	4.7 ± 0.04	12.6 ± 1.2	10.1 ± 0.1	164.3 ± 4	159.7 ± 4.2	18.5 ± 0.2	12.2 ± 0.1
G2	Normal saline	5.7 ± 1	6.3 ± 0.8	4.1 ± 0.3	4.7 ± 0	12.7 ± 1.1	10.4 ± 0.1	264.3 ± 5.4	242.7 ± 5	12 ± 0.04	12 ± 0

SA: *S. aureus*; AC: *A. baumannii*; WBC: white blood cell; RBC: red blood cell; RDW: red cell distribution width; PLT: platelets; PDW: platelet distribution width.

In-vitro assay

Flow cytometry results showed that AgNPs induced cell apoptosis-necrosis depends on AgNP size, concentration and exposure time (Figures 3 and 4). Cells damage due to AgNPs (A) with lower size (20-25 nm) were relatively more than cells exposed to AgNPs (B) (30-35 nm). Both of synthesized AgNPs were more cytotoxic at concentration 0.1 µg/mL. Moreover, cell apoptosis-necrosis in both AgNPs were time depended, since a higher rate of cells damage was observed after 48 h exposure compared to 24 h exposure. Finally, AgNPs (A) were more cytotoxic than AgNPs (B) regarding the same concentration and exposure time.

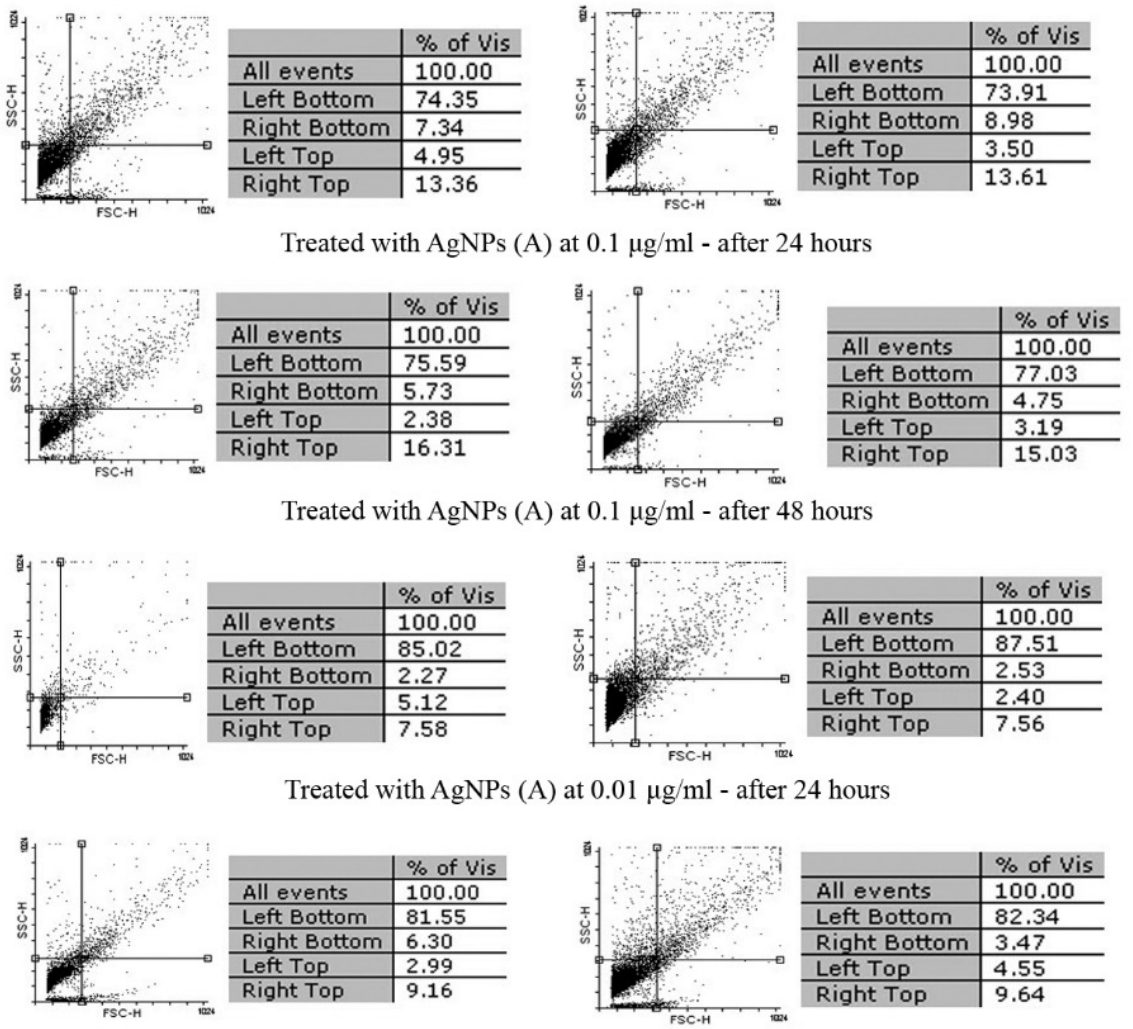

Figure 3. Flow cytometry results of induced cell apoptosis-necrosis by AgNPs (A) (the upper left quadrant represents necrotic cells; the upper right quadrant contains the later apoptotic cells; the lower left quadrant shows viable cells; the lower right quadrant denotes the early apoptotic cells).

Discussion

The increasing production and use of NPs have been associated with the rise of public health concerns regarding their biological safety (28). To our knowledge, few data are available in the literature regarding the *in-vivo* evaluation of NPs biological activity. In this regard, we evaluated related toxicity of our newly synthesized nanochelating based AgNPs at both *in-vitro* and *in-vivo* level.

Depending on the intensity of cellular insult, two types of cell death, necrosis (accidental cell death) and apoptosis (programmed cell death), with different fundamental mechanisms has been introduced (29). Necrotic cells hallmarks are cell and mitochondria swelling resulting in the disruption of cell membranes. In contrast, apoptosis describes a type of cell death characterized by cell shrinkage, nuclear fragmentation, and formation of apoptotic bodies (29). The findings of the present study reveal that cell death caused by exposure to AgNPs is associated with both necrosis and apoptosis. Several different mechanisms can cause NPs intracellular toxicity, but the production of excess reactive oxygen species (ROS) is the most important causes of their cytotoxicity (30). Flow cytometry results showed that regardless of concentration and

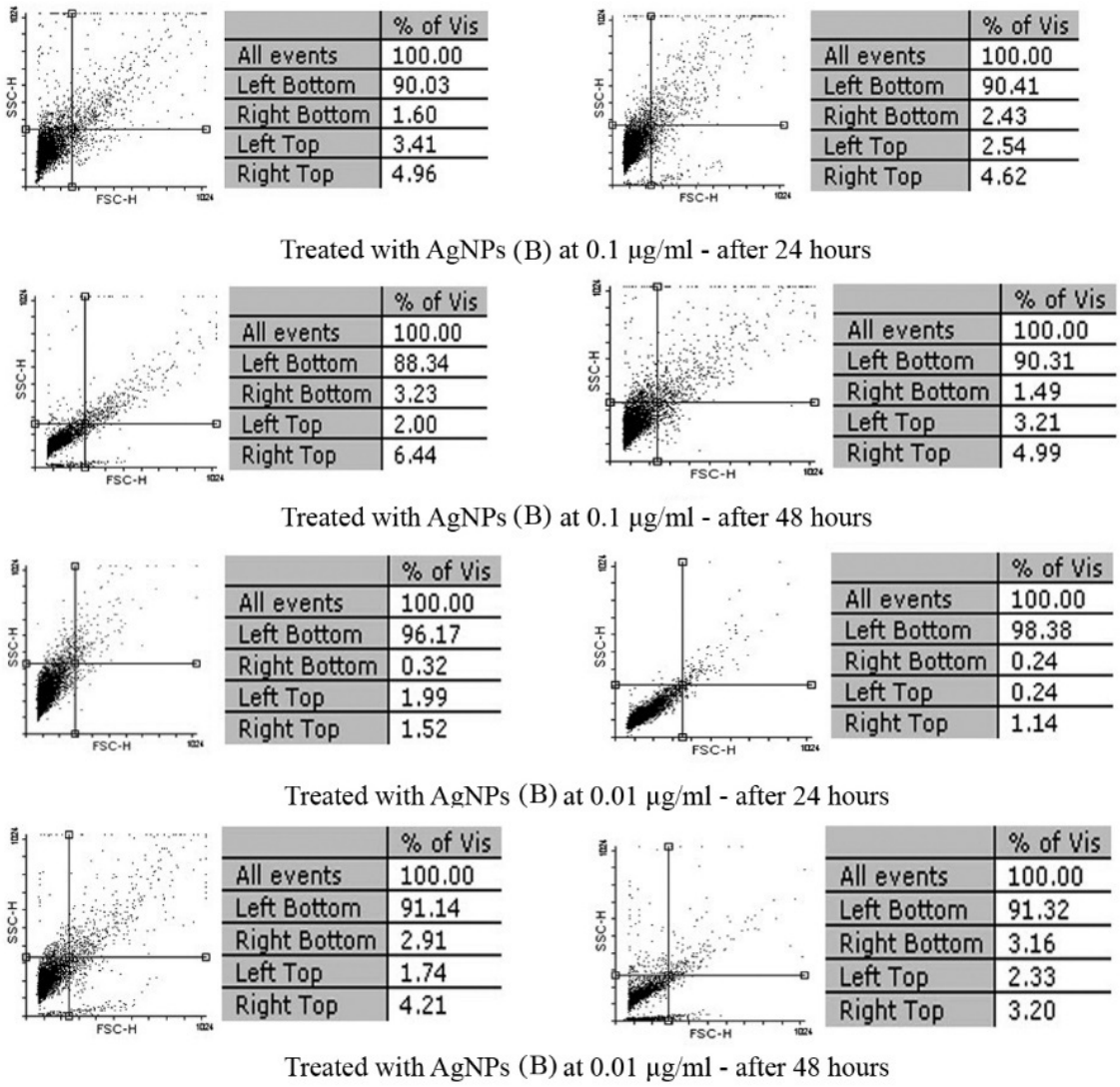

Figure 4. Flow cytometry results of induced cell apoptosis-necrosis by AgNPs (B) (the upper left quadrant represents necrotic cells; the upper right quadrant contains the later apoptotic cells; the lower left quadrant shows viable cells; the lower right quadrant denotes the early apoptotic cells).

exposure time the rate of apoptosis and necrosis in cells treated with AgNPs (A) (2.38-5.1% for necrosis, and 7.56-16.31% for apoptosis) were higher than AgNPs (B) (0.24-3.41% for necrosis, and 1.14-6.44% for apoptosis). Despite the several similar reports with our findings, due to differences in NPs synthesizing methods, structure, and experiment conditions the comparison of newly synthesized NPs is challenging (31-33). For example, Bendale *et al.* showed the rate of apoptosis in the human cancer cells treated with 200 µg/mL of platinum nanoparticles (ptNPs) after 48 h was 8% (31). Kang *et al.* showed the rate of apoptosis in a murine dendritic cell line treated with Polyvinylpyrrolidine-coated AgNPs was up to 2.6% in a concentration-dependent manner (32). Krętowski *et al.* showed the rate of apoptosis in a glioblastoma cell line treated with Silica NPs was aprroximatly 5-70% in a time and dose-dependent manner (33). As a general concept from the previous studies, time and dose of exposure are decisive factors for effects of NPs on apoptosis/necrosis. However, because of differences through the studies, determination of the toxicity effects of each individual newly synthesized NPs is essential. Meanwhile, based on the apoptosis/necrosis results, and considering potential role of AgNPs in cell death regulation, understanding

the association between NPs properties and cell death will assist in designing and developing NPs for biomedical implications, including cancer therapy or autoimmune disorders.

Blood compatibility is an essential property for the evaluation of biological activity of new synthesized NPs and previously by several authors (34-36). Therefore, the blood contact properties of our nanochelating based AgNPs evaluated prior to clinical use to estimate their biological safety. Based on our results no adverse alterations in the blood parameters, and also no sign of liver toxicity by increasing ALT and AST enzymes level were seen. In accordance with our findings, Freese *et al.* showed no obvious effects of 20 nm-sized PEGylated Gold (Au) NPs on endothelial cells after entering the blood stream (34). Yang *et al.* in agreement with our results, showed amphiphilic-polymer coated AgNPs and AuNPs had no significant signs of toxic reactions on weight, liver, and hematology markers (36). In contrast, Huang *et al.* showed AgNPs with two different surface coatings (polyvinyl pyrrolidone and citrate) could elicit hemolysis and severely impact the proliferation and viability of lymphocytes at concentrations 10, 20, and 40 μg/mL (35). Nevertheless, both coated AgNPs didn't show any effect on platelet aggregation, coagulation process, or complement activation at up to ~40 μg/mL (35). Based on previous reports, it is obvious that the NPs chemical composition played a critical role in their *in-vivo* biological activity.

Regard to the antibacterial activity of our synthesized AgNPs at *in-vivo* level, we observed a dose-related healing effects among infected mice received NPs in comparison with controls. Moreover, infected mice received a combination of AgNPs with antibiotics showed a better healing effect in comparison with groups received NPs alone, and controls. One of the prominent implications of antibacterial properties of NPs in the medicine is their healing effect on infected wounds. Previously, several authors showed that different metal-based NPs such as AgNPs, and AuNPs can accelerating the treatment of infected skin wounds (37-40). The results of present study, regarding the healing effect of our newly synthesized AgNPs with no obvious toxicity, support our previous work on antibacterial and antibiofilm activity of AgNPs (21). These findings encourage the use of these newly introduced AgNPs to dealing with the rapid emergence of antimicrobial drug resistance, and the treatment of chronic infections, which are often caused by the formation of biofilms and/or by intracellular microbes.

In our findings, the biological effects of NPs seem to be mostly size and dose-dependent, since AgNPs with different size and surface exhibited distinctive properties. NPs size and surface area are crucial material characteristics from a biological point of view, since the much larger NPs were chemically inert, due to their lower specific surface area (30). A similar observation was cited by Nakhjavani *et al.*, where they showed that green synthesized AgNPs had a great potential for antibacterial activity depending on the size of the particles (41). It has been showed that cellular uptake and efficiency of NPs processing in the endocytic pathway are dependent on the size of the material, therefore size plays a key role in physiological response, distribution, and elimination of materials (30).

Conclusion

In summary, our findings support the potent antibacterial activities of nanochelating based AgNPs as antibacterial agents in infected mice. Also, the present study showed that nanochelating based AgNPs induce a moderate level of apoptosis/necrosis in mice, and affected several clinical parameters like blood parameters, liver enzymes, and body weight with no definite signs of toxicity. We believe this information provided important evidence in the understanding of the biological activity of AgNPs for evaluation in further clinical studies.

Acknowledgment

The manuscript is based on the thesis of Ph.D degree by Seyedeh Mahsan Hoseini-Alfatemi and financially was supported by Shahid Beheshti University of Medical Sciences Research fund (Grant no. 7630).

References

(1) Schabrun S and Chipchase L. Healthcare equipment as a source of nosocomial infection: a systematic

review. *J. Hosp. Infect*. (2006) 63: 239-45.
(2) Brown AN, Smith K, Samuels TA, Lu J, Obare SO and Scott ME. Nanoparticles functionalized with ampicillin destroy multiple-antibiotic-resistant isolates of Pseudomonas aeruginosa and Enterobacter aerogenes and methicillin-resistant Staphylococcus aureus. *Appl. Environ. Microbiol*. (2012) 78: 2768-74.
(3) Heidari H, Hasanpour S, Ebrahim-Saraie HS and Motamedifar M. High incidence of virulence factors among clinical enterococcus faecalis isolates in southwestern Iran. *Infect. Chemother*. (2017) 49: 51-6.
(4) Ghaffarian F, Hedayati M, Sedigh Ebrahim-Saraie H, Atrkar Roushan Z and Mojtahedi A. Molecular epidemiology of ESBL-producing Klebsiella pneumoniae isolates in intensive care units of a tertiary care hospital, North of Iran. *Cell. Mol. Biol (Noisy-le-grand)* (2018) 64: 75-9.
(5) Ebrahim-Saraie HS, Nezhad NZ, Heidari H, Motamedifar A and Motamedifar M. Detection of antimicrobial susceptibility and integrons among extended-spectrum beta-lactamase producing uropathogenic *escherichia coli* isolates in southwestern Iran. *Oman. Med. J*. (2018) 33: 218-23.
(6) Ebrahim-Saraie HS, Heidari H, Khashei R, Edalati F, Malekzadegan Y and Motamedifar M. Trends of antibiotic resistance in staphylococcus aureus isolates obtained from clinical specimens. *J. Krishna. Inst. Med. Sci.* (2017) 6: 19-30.
(7) Fair RJ and Tor Y. Antibiotics and bacterial resistance in the 21st century. *Perspect. Medicin. Chem*. (2014) 6: 25-64.
(8) Soltani B, Heidari H, Ebrahim-Saraie HS, Hadi N, Mardaneh J and Motamedifar M. Molecular characteristics of multiple and extensive drug-resistant Acinetobacter baumannii isolates obtained from hospitalized patients in Southwestern Iran. *Infez. Med*. (2018) 26: 67-76.
(9) Asgharzadeh Kangachar S and Mojtahedi A. The presence of extended-spectrum β-lactamase as a risk factor for MDR in clinical isolation of *Escherichia coli. Trop. Biomed*. (2017) 34: 98-109.
(10) van Duin D and Paterson DL. Multidrug-resistant bacteria in the community: trends and lessons learned. *Infect. Dis. Clin. North. Am*. (2016) 30: 377-90.
(11) Friedman ND, Temkin E and Carmeli Y. The negative impact of antibiotic resistance. *Clin. Microbiol. Infect*. (2016) 22: 416-22.
(12) Tavakoly T, Jamali S, Mojtahedi A, Khan Mirzaei M and Shenagari M. The prevalence of CMY-2, OXA-48 and KPC-2 genes in clinical isolates of Klebsiella spp. *Cell. Mol. Biol (Noisy-le-grand)* (2018) 64: 40-4.
(13) Huh AJ and Kwon YJ. "Nanoantibiotics": a new paradigm for treating infectious diseases using nanomaterials in the antibiotics resistant era. *J. Control. Release* (2011) 156: 128-45.
(14) Franci G, Falanga A, Galdiero S, Palomba L, Rai M, Morelli G and Galdiero M. Silver nanoparticles as potential antibacterial agents. *Molecules* (2015) 20: 8856-74.
(15) Hajipour MJ, Fromm KM, Ashkarran AA, Jimenez de Aberasturi D, de Larramendi IR, Rojo T, Serpooshan V, Parak WJ and Mahmoudi M. Antibacterial properties of nanoparticles. *Trends. Biotechnol*. (2012) 30: 499-511.
(16) Gao W, Thamphiwatana S, Angsantikul P and Zhang L. Nanoparticle approaches against bacterial infections. *Wiley Interdiscip. Rev. Nanomed. Nanobiotechnol*. (2014) 6: 532-47.
(17) Huang L, Dai T, Xuan Y, Tegos GP and Hamblin MR. Synergistic combination of chitosan acetate with nanoparticle silver as a topical antimicrobial: efficacy against bacterial burn infections. *Antimicrob. Agents Chemother*. (2011) 55: 3432-8.
(18) Gholami M, Nazari S, Farzadkia M, Mohseni SM, Matboo SA, Dourbash FA and Hasannejad M. Nano polyamidoamine-G7 dendrimer synthesis and assessment the antibacterial effect *in-vitro*. *Tehran Univ. Med. J*. (2016) 74: 25-35.
(19) Hemeg HA. Nanomaterials for alternative antibacterial therapy. *Int. J. Nanomedicine* (2017) 12: 8211-25.
(20) Nazaran MH. *Chelate compounds*. Google Patents; (2012) https://www.google.com/patents/US20120100372.
(21) Hoseini-Alfatemi SM, Karimi A, Armin S, Fakharzadeh S, Fallah F and Kalanaky S. Antibacterial and antibiofilm activity of nanochelating based silver nanoparticles against several nosocomial pathogens. *Appl. Organomet. Chem*. (2018) 32: e4327.
(22) OECD Guidelines for Testing of Chemicals. Acute Oral Toxicities up and down Procedure. (2001) 425: 1-26.
(23) Cunny H and Hodgson E. Toxicity Testing. In: Hodgson E. *A Textbook of Modern Toxicology*. 3rd ed. John Wiley and Sons Inc. Hoboken, New Jersey (2004) 353-96.
(24) Pitts M and Applied Research Ethics National Association/Office of Laboratory Animal Welfare. Institutional Animal Care and Use Committee. A guide to the new ARENA/OLAW IACUC guidebook. *Lab Anim. (NY)* (2002) 31: 40-2.
(25) Wayne P. Performance standards for antimicrobial susceptibility testing. 26th Informational Supplement. *Clin. Lab. Stand. Ins.* (2016) 2016: 67-81.
(26) Kumar G, Degheidy H, Casey BJ and Goering PL. Flow cytometry evaluation of *in-vitro* cellular necrosis and apoptosis induced by silver nanoparticles. *Food*

Chem. Toxicol. (2015) 85: 45-51.

(27) Riccardi C and Nicoletti I. Analysis of apoptosis by propidium iodide staining and flow cytometry. *Nat. Protoc*. (2006) 1: 1458-61.

(28) Al-Mubaddel FS, Haider S, Al-Masry WA, Al-Zeghayer Y, Imran M, Haider A and Ullah Z. Engineered nanostructures: A review of their synthesis, characterization and toxic hazard considerations. *Arab. J. Chem*. (2017) 10: S376-S88.

(29) Bertho AL, Santiago MA and Coutinho SG. Flow cytometry in the study of cell death. *Mem. Inst. Oswaldo. Cruz*. (2000) 95: 429-33.

(30) Sharifi S, Behzadi S, Laurent S, Forrest ML, Stroeve P and Mahmoudi M. Toxicity of nanomaterials. *Chem. Soc. Rev*. (2012) 41: 2323-43.

(31) Bendale Y, Bendale V and Paul S. Evaluation of cytotoxic activity of platinum nanoparticles against normal and cancer cells and its anticancer potential through induction of apoptosis. *Integr. Med. Res*. (2017) 6: 141-8.

(32) Kang K, Jung H and Lim JS. Cell death by polyvinylpyrrolidine-coated silver nanoparticles is mediated by ROS-dependent signaling. *Biomol. Ther (Seoul)* (2012) 20: 399-405.

(33) Kretowski R, Kusaczuk M, Naumowicz M, Kotynska J, Szynaka B and Cechowska-Pasko M. The effects of silica nanoparticles on apoptosis and autophagy of glioblastoma cell lines. *Nanomaterials (Basel)* (2017) 7: 230.

(34) Freese C, Anspach L, Deller RC, Richards SJ, Gibson MI, Kirkpatrick CJ and Unger RE. Gold nanoparticle interactions with endothelial cells cultured under physiological conditions. *Biomater. Sci*. (2017) 5: 707-17.

(35) Huang H, Lai W, Cui M, Liang L, Lin Y, Fang Q, Liu Y and Xie L. An evaluation of blood compatibility of silver nanoparticles. *Sci. Rep*. (2016) 6: 25518.

(36) Yang L, Kuang H, Zhang W, Aguilar ZP, Wei H and Xu H. Comparisons of the biodistribution and toxicological examinations after repeated intravenous administration of silver and gold nanoparticles in mice. *Sci. Rep*. (2017) 7: 1-12.

(37) Arafa MG, El-Kased RF and Elmazar MM. Thermoresponsive gels containing gold nanoparticles as smart antibacterial and wound healing agents. *Sci. Rep*. (2018) 8: 13674.

(38) Orlowski P, Zmigrodzka M, Tomaszewska E, Ranoszek-Soliwoda K, Czupryn M, Antos-Bielska M, Szemraj J, Celichowski G, Grobelny J and Krzyzowska M. Tannic acid-modified silver nanoparticles for wound healing: the importance of size. *Int. J. Nanomedicine* (2018) 13: 991-1007.

(39) Adibhesami M, Ahmadi M, Farshid AA, Sarrafzadeh-Rezaei F and Dalir-Naghadeh B. Effects of silver nanoparticles on Staphylococcus aureus contaminated open wounds healing in mice: An experimental study. *Vet. Res. Forum* (2017) 8: 23-8.

(40) Ahmadi M and Adibhesami M. The effect of silver nanoparticles on wounds contaminated with pseudomonas aeruginosa in mice: an experimental study. *Iran. J. Pharm. Res*. (2017) 16: 661-9.

(41) Nakhjavani M, Nikkhah V, Sarafraz MM, Shoja S and Sarafraz M. Green synthesis of silver nanoparticles using green tea leaves: Experimental study on the morphological, rheological and antibacterial behaviour. *Heat Mass Tran*. (2017) 53: 3201-9.

This article is available online at http://www.ijpr.ir